Journal of Power Sources 220 (2012) 292–297

Contents lists available at SciVerse ScienceDirect

Journal of Power Sources

journal homepage: www.elsevier.com/locate/jpowsour

A dual-chambered microbial fuel cell with Ti/nano-TiO_2/Pd nano-structure cathode

Mir Ghasem Hosseini*, Iraj Ahadzadeh

Electrochemistry Research Laboratory, Department of Physical Chemistry, Faculty of Chemistry, University of Tabriz, 29 Bahman Blv., Tabriz 5166616471, Iran

HIGHLIGHTS

- A new cathode using the benefits of titanium dioxide (TiO_2) nano-structures.
- Application of electrochemical impedance to monitor the cell performance.
- Electrocatalytic activity of palladium nanoparticles.

ARTICLE INFO

Article history:
Received 7 April 2012
Received in revised form
3 July 2012
Accepted 31 July 2012
Available online 8 August 2012

Keywords:
Microbial fuel cell (MFC)
Mixed-culture biofilm
Nano-structured cathode
Electrochemical impedance spectroscopy (EIS)
Oxygen reduction reaction
Cation exchange membrane

ABSTRACT

In this research, Ti/nano-TiO_2/Pd nano-structure electrode is prepared, characterized and applied as cathode electrode in a dual-chambered microbial fuel cell with graphite anode and Flemion cation exchange membrane. Prepared nano-structured electrode morphology and mixed-culture biofilm formed on the anode are studied by scanning electron microscopy (SEM). Cell performance is investigated by polarization, cyclic voltammetery (CV) and electrochemical impedance spectroscopy (EIS) methods. Results show that Ti/nano-TiO2/Pd electrode exhibits satisfactory long term performance as a cathode to reduce water dissolved oxygen. The maximum output power of the cell is about 200 mW m^{-2} normalized to the cathode surface area. Open circuit potential (OCP) of the cell is about 480 mV and value of the short circuit current is 0.21 mA cm^{-2} of the cathode geometric surface area. Thus this nano-structure cathode can produce comparable output power to that of platinum-based cathodes such as Pt-doped carbon paper; therefore due to the ease of preparation and low cost, this electrode can be applied as alternative to platinum-based cathodes in microbial fuel cells.

1. Introduction

Microbial fuel cells (MFCs) harvest electric energy from organic matter by microorganism assisted oxidation of biodegradable materials [1,2]. However, at this time, mainly due to slow reaction kinetics and high internal ohmic losses, power output level of these fuel cells is very low compared to other electricity generation technologies [3–6]. Gaining insight to and deep understanding of electrochemical processes taking place at the surface of both anode and cathode electrodes as well as the kinetic and/or mass transfer factors limiting the output power through well developed electrochemical methods is of great importance for further development of these novel energy conversion devices [7–9]. For an MFC to be economical and efficient some barriers are still needed to be overcome, one of those is the low power level which mainly results from losses due to high internal resistance of an MFC system [10–12]. One of the main problems in the development of this novel technology is the design and construction of effective catalysts to reduce water dissolved oxygen as cathodic electron acceptor [13–15]. Cathodes based on precious materials and metals such as carbon paper and platinum are promising for this purpose but they are expensive beyond to be practically used in large scale applications [16,17]. In this research palladium was deposited on inner walls of TiO_2 nanotubes prepared through anodizing a titanium electrode and prepared Ti/nano-TiO_2/Pd electrode was employed as a cathode in a dual-chambered microbial fuel cell with graphite anode. Prepared nano-structured electrode morphology was studied by scanning electron microscopy (SEM). Glucose and anaerobic activated sludge were as organic feed and mixed-culture bacterial medium, respectively. Cell performance was investigated by polarization and electrochemical impedance spectroscopy (EIS) methods.

* Corresponding author. Tel.: +98 4113393138; fax: +98 4113340191.
E-mail address: mg-hosseini@tabrizu.ac.ir (M.G. Hosseini).

0378-7753/$ – see front matter © 2012 Elsevier B.V. All rights reserved.
http://dx.doi.org/10.1016/j.jpowsour.2012.07.096

2. Materials and methods

2.1. Chemicals and fuel cell setup

Fig. 1 shows the microbial fuel cell setup employed in this research. This homemade configuration consists of two polycarbonate plastic cylinders each of about 125 cm^3 volume with a 3 cm wide O-ring fitted aperture between them to set a 3.1 cm^2 area Flemion cation exchange membrane (250 μm thickness, provided by Asahi Glass Company, Japan). Anode in the shape of a rectangle with a total geometrical area of 24.3 cm^2 was made of commercial electrical grade graphite plate. Distance between cathode and anode was 8.5 cm. All chemicals used throughout the study were of analytical grade provided by Merck (Germany) and used as received without any further treatment. Double distilled water was used to all solution preparation and rinse purposes.

2.2. Preparation of the anode

Before initiation of the experiments, fuel cell setup was immersed in a $KMnO_4$ solution (3 $g\,L^{-1}$) for 24 h in order to disinfect the anode and cathode chambers prior to any bacterial inoculation in the anode compartment. After three times rinse with double distilled water, cation exchange membrane was fitted between anodic and cathodic parts using three stainless steel screws. Electrolyte composition was as follow: 60 mM biological phosphate buffer solution (PBS) with pH = 7.4, $MgSO_4$ (0.9 $g\,L^{-1}$) and NH_4Cl (1 $g\,L^{-1}$) and 0.1 $mL\,L^{-1}$ trace essential elements solution (contained per liter: 23 mg $MnCl_2{\cdot}2H_2O$, 30 mg $MnCl_4{\cdot}H_2O$, 31 mg H_3BO_3, 36 mg $CoCl_2{\cdot}6H_2O$, 10 mg $CuCl_2{\cdot}2H_2O$, 20 mg $NiCl_2{\cdot}6H_2O$, 50 mg $ZnCl_2$, and 30 mg $Na_2MoO_4{\cdot}2H_2O$). Prior to the insertion of the graphite anode into the anolyte, the biofilm was formed on graphite anode in a batch procedure as follows: the graphite anode was immersed in a solution with the composition of the anolyte along with 1 $g\,L^{-1}$ glucose ($C_6H_{12}O_{11}$) as feed and 1 mL of urban waste water (Tabriz) sludge as mixed-culture bacterial source, while kept stirring for 24 h in anaerobic conditions. Anaerobic conditions were achieved by bubbling pure nitrogen gas into the solution for 0.5 h then the setup was kept sealed using proper gas tight miniature taps. Stirring was used to produce a gentle sheer on the surface of the anode with the hope of obtaining a more compact and active biofilm. After fitting the anode covered with biofilm and adding 100 mL of the anolyte solution containing 1 $g\,L^{-1}$ glucose into the anodic section, anaerobic condition was further observed in that compartment by sealing all apertures around the anode by water-proof silicone sealant. The cathodic chamber was air-bubbled by an air-stone dispenser at a rate of 1 $L\,min^{-1}$ using an aquarium fish pump. Whole of the cell was kept at room temperature of $23 \pm 1\,^{\circ}C$ throughout the study.

2.3. Preparation of the cathode

Cathode electrode was prepared by electroless deposition of palladium on inner walls of TiO_2 nanotubes formed through anodizing of a titanium electrode [18]. Self-organized, vertically oriented and uniformly distributed TiO_2 nanotube arrays on a pure titanium substrate (TiO_2 nanotube/Ti electrode) were prepared by anodizing of pure titanium sheet in a non-aqueous fluoride-containing electrolyte. Titanium cathode in the shape of a rectangle having an area of 15 cm^2 was cut from a titanium sheet (purity 99.99%, 1 mm thickness) and degreased by sonicating in acetone and ethanol followed by rinsing with distilled water. Anodic TiO_2 films were grown from titanium by potentiostatic anodizing in an ethylene glycol electrolyte containing 25×10^{-4} %W/V NH_4F at a constant voltage of 40 V using a platinum sheet as counter electrode. After anodizing of titanium, the cathode was ultrasonically cleaned in distilled water for 5–10 min to remove surface contaminants. Palladium nanoparticles were deposited on the nanotubes by electroless method [19]. After the electroless plating, the cathode was rinsed, dried and subjected to the characterization. Morphology, alignment, and composition of the TiO_2 nanotube array and palladium coating on TiO_2 nanotubes matrix were characterized with a scanning electron microscope (Philips, Model XL30). The same apparatus was employed to study the mixed-culture biofilm formed on the graphite anode. Fig. 2 shows the SEM micrograph of the prepared $Ti/TiO_2/Pd$ electrode which was employed as cathode. Fig. 3 shows the SEM micrograph of the biofilm formed on the anode in the culture media after 24 h inoculation. The nano-structure electrode prepared in this way and similar electrodes have previously been studied as an electro-active catalytic substrate for the electro-oxidation of a variety of organic materials such as methanol and its high catalytic activity is well proven at least for the studied chemicals, so it can be expected that this modified electrode can potentially be applied for the oxygen reduction reaction at the cathode [20,21].

$$\text{at the cathode}: O_2(\text{dissolved}) + 4H^+(\text{produced at anode}) + 4e \rightarrow 2H_2O \quad (1)$$

2.4. Polarization measurements

Polarization measurements were performed by successive lowering the value of an externally connected homemade precision-resistor box to the anode and cathode via some length of wire and two crocodile clamps, and at the same time recording the potential drop across the load resistor. Variation range of the resistor box was from 2 MΩ to 10 Ω in a logarithmic scale. All potential records were performed using a high input impedance (10 MΩ) commercial 3.5 digit voltmeter. Sufficient time interval, typically 5 min, was observed after each change in resistor box value to obtain a stable potential reading. Short circuit current was measured using a 3.5 digit commercial ammeter with 200 μA full range.

2.5. Cyclic voltammetery (CV)

Cyclic voltammetery is one of the most robust electrochemical techniques to study red-ox reaction kinetics at the electrode/electrolyte interface [22]. In this study, this method was used to study the oxygen reduction reaction at the prepared cathode/catholyte interface. After 36 h work of the cell using a 1000 Ω external resistor, cyclic voltammetery studies were performed for the cathode using an EG&G Princeton applied Research Parstat 2263 advance Electrochemical System (USA) in two successive cycles in the potential range of −1.5 V to 1.5 V versus saturated calomel electrode (SCE) at 25 $mV\,s^{-1}$ potential scan rate. In order to record cyclic voltammograms, the working and counter terminal of the electrochemical instrument were connected to the cathode and anode, respectively while a saturated calomel electrode was inserted into the cathodic compartment, i.e. a three-electrode configuration was adopted.

2.6. Electrochemical impedance spectroscopy

Electrochemical impedance spectroscopy (EIS) is a powerful technique recently being applied to study fuel cell systems in

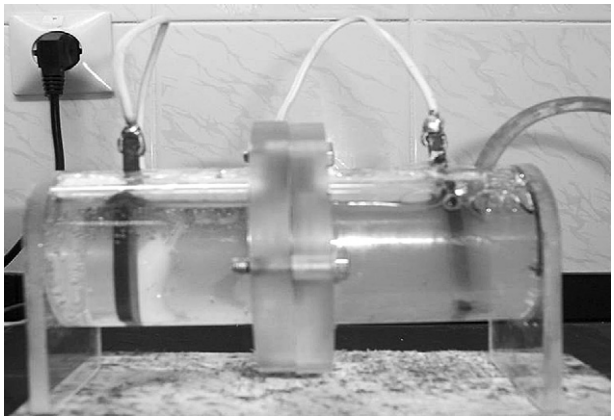

Fig. 1. Dual-chambered microbial fuel cell setup.

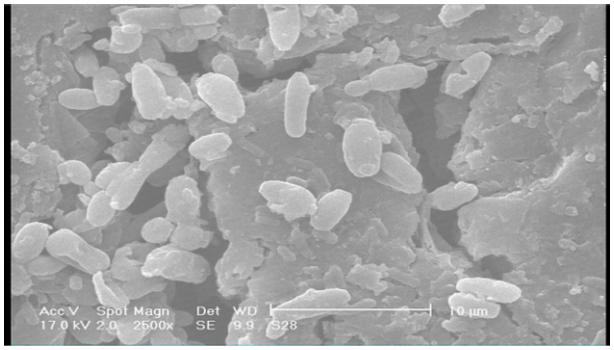

Fig. 3. SEM micrograph of the mixed-culture biofilm on the graphite anode electrode.

general and MFCs in particular [23,24]. Electrochemical impedance spectrum was recorded at different operation intervals using an EG&G Princeton applied Research Parstat 2263 advance Electrochemical System (USA) from frequency of 100 kHz down to 0.01 Hz at open circuit (external resistor load disconnected) condition. Impedance measurements were performed for the anode, cathode, and whole of the microbial fuel cell. In order to measure impedance of the anode, the working and counter terminal of the EIS instrument were connected to the anode and cathode, respectively while a saturated calomel electrode (SCE) was inserted into the cathodic compartment, i.e. a three-electrode configuration was adopted. The same procedure was repeated for the cathode impedance measurement but the connections of the working and counter terminals reversed. To measure the impedance of whole microbial fuel cell, use was made of a two-electrode configuration in which counter and reference electrodes of the impedance measuring apparatus were connected to the cathode and working electrode was electrically fixed to the anode of the fuel cell.

2.7. Coulombic efficiency

While generating power is a main goal of MFC operation, to extract as much of the electrons stored in the biomass as possible as current, and to recover as much energy as possible from the system is also of great desire. The recovery of electrons is referred to as coulomb efficiency, defined as the fraction (or percent) of electrons recovered as current versus that in the starting organic matter. Coulombic efficiency, CE, is defined as: CE = Coulombs recovered/total coulombs in substrate.

An ampere is defined as the transfer of 1 Coulomb of charge per second, or 1 A = 1 CIS. Thus, if we integrate the current obtained over time we obtain the total Coulombs transferred in our system. The CE can therefore be calculated for a fed-batch system as [2]

$$\mathrm{CE} = \frac{M_s \int_0^{t_b} I\,\mathrm{d}t}{F b_{es} v_{An} \Delta c} \tag{2}$$

where Δc is the substrate concentration change over the batch cycle which is usually assumed to go from c_0, the starting concentration, to completion for defined substrates such as glucose, or $\Delta c = c_0 - c = c_0 - 0 = c_0$ over a time $= t_b$, M_s, is the molecular weight of the substrate, F = Faraday's constant, and v_{An} is the volume of liquid in the anode compartment. The parameter b_{es} indicates the number of electrons released during complete oxidation of the substrate. Therefore, in this study, v_{An}, Δc, M_s and b_{es} are 0.1 L, 5.55×10^{-4} M, 180 g mol^{-1} and 24 electron, respectively, because the oxidation reaction of glucose involves a 24 electron release process:

$$6H_2O + C_6H_{12}O_6 \rightarrow 6CO_2 + 24H^+ + 24e \tag{3}$$

In order to calculate coulomb efficiency, a freshly prepared cell with 0.1 g L^{-1} glucose feed was externally connected to a 10 Ω resistor and the potential drop on that resistor was continually recorded for 168 h. Dividing the potential drop (in volts) by the resistor (value in Ohms) gives the current produced by the cell at a given time. So the plot of current versus time can be constructed and through fitting the resulted curve with a suitable mathematical function and integrating to calculate the area under curve (i.e. charge passed in coulombs) using TableCurve™ mathematical software, coulomb efficiency can be calculated.

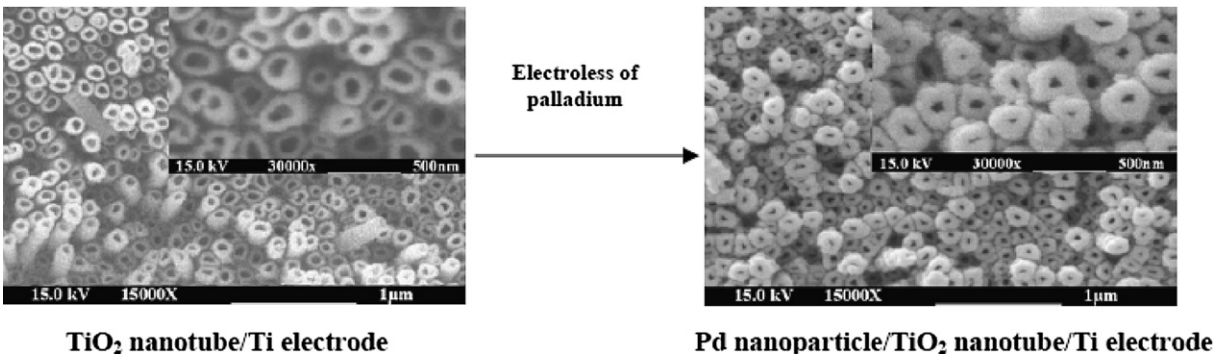

Fig. 2. SEM micrograph of Ti/TiO_2/Pd electrode employed as cathode.

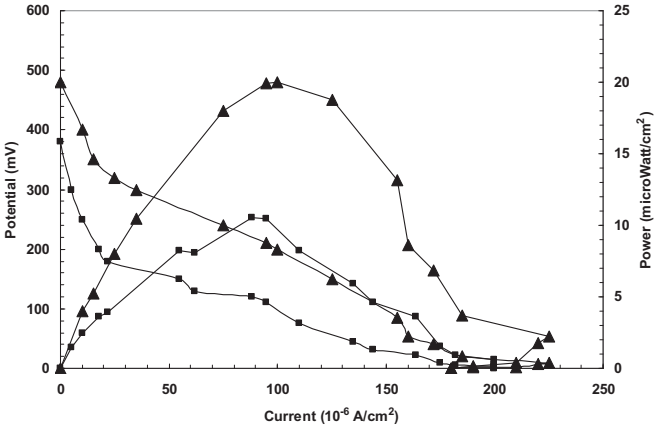

Fig. 4. Polarization (potential and power) curves of microbial fuel cell after 9 h (■) and 36 h (▲) operation with a 1000 Ω external resistor.

3. Results and discussions

3.1. Characterization of the prepared nano-structure cathode

Scanning electron microscopy (SEM) images of a typical TiO_2 nanotube array and nanotubes after loading with Pd nanoparticles using electroless approach are shown in Fig. 2. From Fig. 2, it can be seen that TiO_2 nanotubes are well aligned and organized into a highly oriented array. From the inset of the enlarged image, the average diameters of these tubes are found to be about 70–90 nm. It can be seen that the palladium nanoparticles with diameters around 20–30 nm are distributed in an almost homogeneous manner on the surface of the TiO_2 nanotubes. So, SEM images confirm the nano-structure of the prepared cathode electrode.

3.2. Polarization measurements

Fig. 4 shows the voltage–current (V–I) and power–current (P–I) polarization curves of the cell after 9 and 36 h of the cell operation with 1000 Ω external resistor. As can be seen from Fig. 4, the maximum output power of the cell is about 200 mW m^{-2} normalized to the cathode surface area which equals to about 120 mW m^{-2} of the anode geometric surface area because the ratio of the surface area of the cathode to the anode was about 0.6 in this study. Open circuit potential (OCP) of the cell is about 480 mV and value of the short circuit current is 0.21 mA cm^{-2} of the cathode geometric surface area which equals to 0.13 mA cm^{-2} of the anode geometric surface area. This output power level is comparable with those reported for other rather similar MFC setups in the literature,

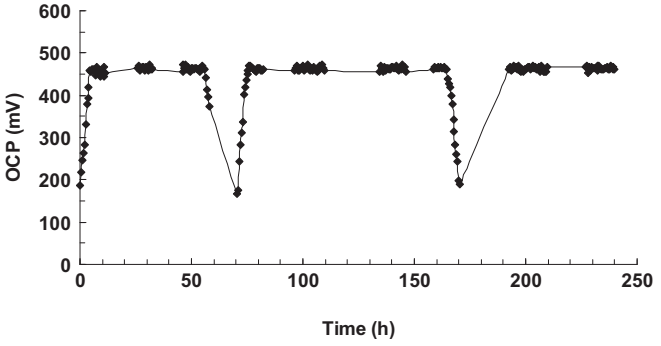

Fig. 5. Cell open circuit potential (OCP) variation versus time.

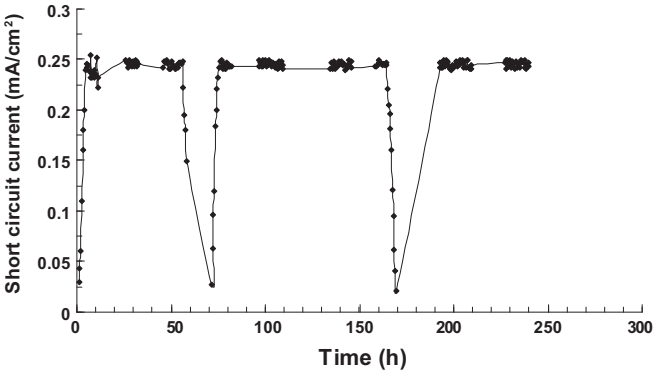

Fig. 6. Cell short circuit current trend versus time.

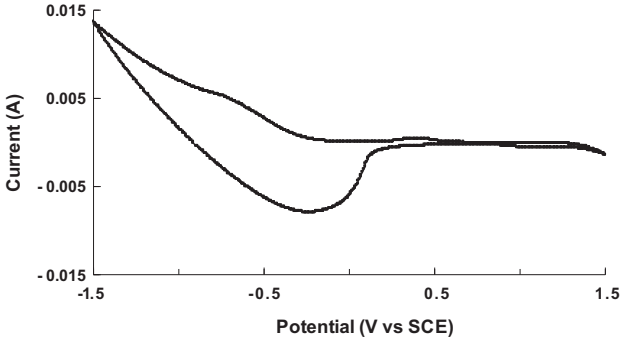

Fig. 7. Cyclic voltammograms of the cathode.

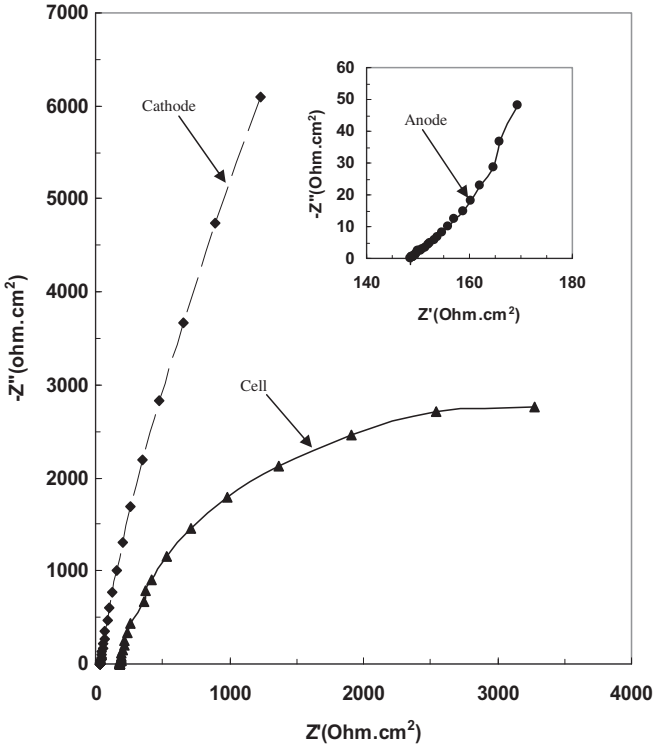

Fig. 8. Fitted Nyquist impedance spectra of anode, cathode, and whole of the microbial fuel cell after 36 h work with 1000 Ω external resistance.

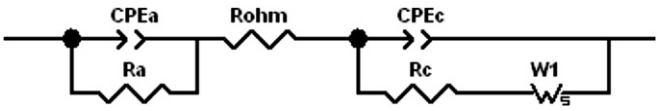

Fig. 9. Electrical equivalent circuit (EEC) for analysis of EIS spectra.

i.e. 309 mW m^{-2} for anode surface area with Pt-doped carbon cloth (0.5 mg, 10% Pt) [26], 3.9 mW m^{-2} again normalized to anode surface area for solid graphite cathode [27] and 64.7 mW m^{-2} for CoNPc/C (Co-naphthalocyanine catalyst on carbon) cathode, 81.3 mW m^{-2} of Pt/C (platinum coated carbon) cathode and 9.3 mW m^{-2} of carbon black [28].

Also in a subsequent complementary study, all conditions mentioned so far were maintained fixed for this MFC setup with the exception that a platinum sheet with a geometric area of 24 cm^2 was employed as cathode electrode. Polarization results showed that a maximum power of 235 mW m^{-2} of cathode surface area and 141 mW m^{-2} of anode surface area can be obtained after 36 h of cell operation (detailed data not reported here). Internal resistance of an MFC is the main factor affecting the output power of the cell. The lower the internal resistance, the higher the output power will be. Internal resistance has three major components, i.e. **a)** kinetic charge transfer resistance of the cathodic and anodic reactions at low currents, **b)** ohmic resistance of the electrolytes and membranes at medium currents and **c)** mass transfer limitations of the reactants toward anode and cathode at high current ranges. Internal resistance can be measured or calculated by different methods such use of polarization data, EIS, current interruption method [2]. Internal ohmic resistance of the cell was calculated as the slope of the linear segment of the *V–I* curve at medium range currents through fitting the experimental *V–I* data on a linear equation [2]. Calculated internal resistances were about 8900 Ω after 9 h and 5100 Ω after 36 h of cell operation.

Also trends in the cell open circuit potential and short circuit current are shown in Figs. 5 and 6, respectively. The sudden fall and subsequent rise in the potential and current values are correspond to the consumption of the glucose feed in the anodic chamber followed by insertion of fresh 1 g L^{-1} glucose feed solution. It should be mentioned that due to large electrical load imposed on the cell during short circuit conditions, immediately after each measurement of the short circuit current, cell was allowed to work with highest external resistor (2 MΩ) for a sufficient time, typically 20 min, to reach the previous steady state ready to other subsequent polarization measurements.

3.3. Cyclic voltammetery (CV)

Two successive cyclic voltammograms of the cathode are shown in Fig. 7. As it is evident from Fig. 7, a reduction peak can be observed for both cycles at the potential of about −400 mV about versus SCE which can be attributed to the reduction of water dissolved oxygen at the cathode electrode, because according to the composition of the catholyte no other electro-active species is present in the catholyte. On the other hand, no relevant oxidation peak is present in the anodic scan. So it seems that the main cathodic reaction in this setup is the irreversible water dissolved oxygen reduction to form water (Eq. (1)).

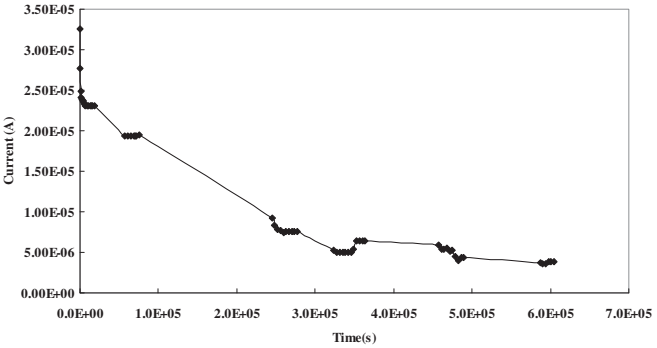

Fig. 10. The plot of current versus time (*I–t* curve) for coulomb efficiency measurement with 10 Ω external load.

3.4. Electrochemical impedance spectroscopy

Nyquist complex impedance plot of anode, cathode and whole of the fuel cell was shown in Fig. 8. Performance parameters such as internal ohmic resistance (*Rint*) i.e. resistance of the anolyte and catholyte solutions and membrane toward transfer of H^+ produced at the anode to the cathode, cathodic and anodic respective charge transfer resistances (R_c and R_a) and their corresponding electrical double layer pseudo-capacitances (Constant Phase Elements i.e. *CPEc* and *CPEa*) were extracted after fitting of the impedance data on the circuit shown in Fig. 9 which is the system's electrical equivalent circuit. This electrical equivalent circuit was designed on the basis of physicochemical model of the fuel cell composed of a cathode electrode and an anode electrode both in contact with electrolyte solution separated by a membrane [25]. Table 1 shows the values of electrical circuit elements derived by fitting the experimental data on the electrical equivalent circuit of the Fig. 9. Fitting and analysis of the EIS data were performed by ZSim™ software. As it can be seen from Table 1, the *CPEc-T* value which is an indication of the cathode/solution interface capacitance magnitude is far greater than *CPEa-T* of the anodic counterpart. With great confidence, this can be attributed to the much higher real surface area of the cathode due to the formation of nanotubes which has its basis in the nano-structural properties of the novel cathode prepared. On the other hand, the value of the *CPE-n* parameter which is inversely proportional to the non-homogeneity and roughness of the electrodes surface is lower for the cathode in a direct accordance to the rough nanotube array formed on the cathodes surface [29]. Value of the cathodic charge transfer resistance for the cathode/electrolyte interface (R_c) which is inversely proportional to the oxygen reduction rate is much greater than the charge transfer resistance of glucose oxidation reaction by bacteria at the anode (R_a). This can be expressed in terms of low solubility of oxygen in water (concentration of about 0.2 mM at ambient temperature) which severely limits the concentration of dissolved oxygen in catholyte compared with glucose concentration in the anolyte solution which, in this study, is around 4.4 mM. Although, in addition to low solubility of oxygen in water, we are dealing with a complex three phase co-existence at the cathodic compartment, i.e. solid cathode electrode/oxygen gas/aqueous H^+ interfaces. So as is well understood, much remains to be done to find efficient and economic cathodic materials [2]. According to the equivalent

Table 1
Electrochemical impedance parameters of cell after 36 h work with 1000 Ω external resistance.

Parameter	R_s (Ω)	R_c (Ω cm^2)	R_a (Ω cm^2)	*CPEa-T*	*CPEa-P*	*CPEc-T*	*CPEc-P*	W-T	W-P
Value	225.3	4753.1	522.8	0.000012	0.92	0.000742	0.81	0.11	0.5

Table 2
Operational parameters of the studied MFC setup.

Parameter	OCP (mV)	I_{sc} (mA cm^{-2})	Power (mW m^{-2})	Internal resistance (Ω)	Coulomb efficiency (%)
Value	480 (after 9 h)	0.21 (normalized to cathode area)	200 (normalized to cathode area)	8900 (after 9 h)	18.6
	480 (after 36 h)	0.13 (normalized to anode area)	120 (normalized to anode area)	5477 (from EIS after 36 h) 5100 (from polarization after 36 h)	

electrical circuit shown in Fig. 9, from impedance data given in Table 1, internal resistance of the cell was calculated as the total sum of the cathodic and anodic polarization resistances (R_c and R_a) and electrolytes and membrane ohmic resistances (R_s). Calculated internal resistance was 5447 Ω at 36 h. So, it can be seen that the internal resistance as calculated from impedance data is in good agreement with the internal resistance value obtained from polarization method.

3.5. Coulomb efficiency

Fig. 10 depicts the plot of current versus time (I–t curve). The equation corresponding to the best fitting of the I–t experimental data extracted by TableCurve™ software is as follows:

$$I(\mathrm{A}) = 2.62 \times 10^{-4} \exp\left(-8.11 \times 10^{-6} t(\mathrm{s})\right) \quad (4)$$

in which A and s symbols stand for ampere and second, respectively.

Integrating the above equation from $t = 0$ s to $t = 604{,}800$ s (i.e. 168 h) and employing the Eq. (4), coulomb efficiency was calculated to be about 18.6%. The value obtained for columbic efficiency is comparable with others reported in the literature [2]. But the rather low CE is a direct indication of the fact that some non-exoelectrogeneous bacteria are present in the mixed-culture medium consuming glucose feed through some alternative biological pathways other than glucose oxidation, such as incomplete fermentation and etc. which is an intrinsic characteristic of waste water mixed culture containing so diverse species of microorganisms [2]. Further growth of the suspended bacteria in the bulk of the anolyte which are not attached to the anode so cannot transfer electrons to it and thus consuming the feed in non-electrogeneous processes can be another possible factor lowering the coulomb efficiency. In summary, Table 2 gives the values of relevant operational parameters of this MFC setup.

4. Conclusions

Results showed that due to high specific surface area of the nano-structured cathode along with its higher palladium electrocatalytic activity toward oxygen reduction reaction in the cathodic part of the MFC, comparable output power to that of platinum-based cathodes such as Pt-doped carbon paper as well as excellent long term performance can be obtained. Therefore due to its ease of preparation i.e. by anodizing titanium and then electroless plating of palladium on the resultant nanotube arrays by an easy electrochemical procedure and also low cost of titanium substrate and palladium electroplating bath materials compared with platinum-based cathode preparation procedures, this electrode can be easily and economically prepared in laboratory in small to medium scales and used as a potential alternative to Pt-based cathodes in microbial fuel cell applications. On the other hand, very satisfactory correlation was found between internal ohmic resistance measured by EIS and that of obtained by time consuming polarization method. Also, from impedance spectra analysis it was found that the role played by kinetic and mass transfer phenomena can easily be resolved for anodic and cathodic half-cell reactions. Therefore EIS reveals itself as a promising electrochemical tool to study and trace the effect(s) of any modification and/or enhancement of construction materials on the power density and long term performance of microbial fuel cell systems.

Acknowledgments

The authors would like to acknowledge the financial support of Iranian Nanotechnology Society and the Office of Vice Chancellor in Charge of Research of University of Tabriz.

References

[1] A. Dewan, C. Donovan, D. Heo, H. Beyenala, J. Power Sources 195 (2010) 90–96.
[2] M.H. Kim, I.J. Iwuchukwu, Y. Wang, D. Shin, J. Sanseverino, P. Frymier, J. Power Sources 196 (2011) 1909–1914.
[3] J.M. Morris, P.H. Fallgren, S. Jin, Chem. Eng. J. 153 (2009) 37–42.
[4] P.Y. Zhang, Z.L. Liu, J. Power Sources 195 (2010) 8013–8018.
[5] G.C. Gil, I.S. Chang, B.H. Kim, M. Kim, J.K. Jang, H.S. Park, H.J. Kim, Biosens. Bioelectron. 18 (2003) 327–334.
[6] Q. Denga, X. Li, J. Zuo, A. Ling, B.E. Logan, J. Power Sources 195 (2010) 1130–1135.
[7] L. Huang, X. Chai, S. Cheng, G. Chen, Chem. Eng. J. 166 (2011) 652–661.
[8] M.D. Lorenzo, K. Scott, T.P. Curtis, I.M. Head, Chem. Eng. J. 156 (2010) 40–48.
[9] M. Grzebyk, G. Pozniak, Sep. Purif. Technol. 41 (2005) 321–328.
[10] P. Liang, X. Huang, M.Z. Fan, X.X. Cao, C. Wang, Appl. Microbiol. Biotechnol. 77 (2007) 551–558.
[11] S. Cheng, H. Liu, B.E. Logan, Environ. Sci. Technol. 40 (2006) 2426–2432.
[12] P. Liang, M.Z. Fan, X.X. Cao, X. Huang, C. Wang, Chin. J. Environ. Sci. 28 (2007) 1894–1898.
[13] F. Zhao, F. Harnisch, U. Schroeder, F. Scholz, P. Bogdanoff, I. Herrmann, Environ. Sci. Technol. 40 (2006) 5193–5199.
[14] H. Wang, Z. Wu, A. Plaseied, P. Jenkins, L. Simpson, C. Engtrakul, Z. Ren, J. Power Sources 196 (2011) 7465–7469.
[15] H. Rismani-Yazdi, S.M. Carver, A.D. Christy, O.H. Tuovinen, J. Power Sources 180 (2008) 683–694.
[16] S. Cheng, H. Liu, B.E. Logan, Environ. Sci. Technol. 40 (2006) 364–369.
[17] G. Zhang, Q. Zhao, Y. Jiao, J. Zhang, J. Jiang, N. Ren, B.H. Kim, J. Power Sources 196 (2011) 6036–6041.
[18] M.G. Hosseini, M.M. Momeni, M. Faraji, Electroanalysis 22 (2010) 2620–2625.
[19] M.G. Hosseini, M. Faraji, M.M. Momeni, Thin Solid Films 519 (2011) 3457–3461.
[20] M.G. Hosseini, M.M. Momeni, J. Mater. Sci. 45 (2010) 3304–3310.
[21] M.G. Hosseini, M.M. Momeni, M. Faraji, J. Mol. Catal. A: Chem. 335 (2011) 199–204.
[22] P.S. Kishore, B. Viswanathan, T.K. Varadarajan, J. Nanosci. Nanotechnol. 9 (2009) 5188–5197.
[23] Z. He, N. Wagner, S.D. Minteer, L.T. Angenent, Environ. Sci. Technol. 40 (2006) 5212–5217.
[24] J.W. Guo, Z.Q. Mao, J.M. Xu, Chem. J. Chin. Univ. 24 (2003) 1477–1481.
[25] B. Min, B.E. Logan, Environ. Sci. Technol. 38 (2004) 4900–4904.
[26] M. Lanthier, K.B. Gregory, D.R. Lovley, Microbiol. Lett. 278 (2007) 29–35.
[27] J.R. Kim, J.Y. Kim, S.B. Han, K.W. Park, G.D. Saratale, S.E. Oh, Bioresour. Technol. 102 (2011) 342–347.
[28] S. Ouitrakul, M. Sriyudthsak, S. Charojrochkul, T. Kakizono, Biosens. Bioelectron. 23 (2007) 721–727.
[29] E. Barsoukov, J.R. Macdonald (Eds.), Impedance Spectroscopy, Theory Experiment and Applications, Wiley Interscience, Chichester, 2005.